




Blocks size effect on the shear strength of bimsoils with low volumetric blocks proportion

Efecto del tamaño de bloques en la resistencia al corte de suelos con bloques (bimsoils) de bajas proporciones volumétricas

Campos-Muñoz., D.D. ¹, Ramos-Cañón., A.M. ², and Prada-Sarmiento., L.F. ³

Fecha de Recepción: 30 de enero de 2023

Fecha de Aceptación: 1 de septiembre de 2024

Cómo citar: Campos-Muñoz., D.D., Ramos-Cañón., A.M. y Prada-Sarmiento., L.F. (2024). Blocks size effect on the shear strength of bimsoils with low volumetric blocks proportion. *Tecnura*, 28(81), 30-53. <https://doi.org/10.14483/22487638.20418>


Abstract

The term bimsoils is used to define the inclusion of rigid blocks embedded in a weak soil matrix, where the stiffness ratio between both materials is greater than two. Research on bimsoils primarily focuses on determining shear strength parameters based on the volumetric proportion of blocks (VBP). However, the shear strength of bimsoils is also influenced by other variables, including the size of the blocks. Although some authors indicate that size has no influence on shear strength, others conclude that strength is greater when the size distribution is well-graded, and the maximum block size is greater. This study analyses the influence of block size and VBP on bimsoils strength parameters, from drained triaxial tests modeled in ABAQUS. The block size is unique in the entire specimen and corresponds to a fraction of the diameter of the sample (D) that varies from 0.1 to 0.2. Shear strength is higher for bimsoils with higher VBP and block size between $0.12D$ and $0.15D$ and it is reflected in the strength parameters. The influence of size occurs for different VBP and when the blocks have a uniform and columnar location. The increment in the VBP generates the increase in the anisotropy of the magnitude of the principal stresses in the sample and the block sizes $0.12D$ and $0.15D$ generate a greater heterogeneity of the shear stresses reflected in the magnitude and propagation of the stresses in the sample.

Keywords: bimsoils, blocks size, drained triaxial test, FEM, volumetric blocks proportion

¹Magister en ingeniería civil de la Pontificia Universidad Javeriana .

Email: dianet912@gmail.com

²Profesor Asociado Universidad Nacional de Colombia .

Email: amramosc@unal.edu.co

³Assistant Professor, Department of Civil and Architectural Engineering, Aarhus University, Denmark .

Email: felipe.prada@cae.au.dk

Resumen

El término bimsoils se utiliza para definir la inclusión de bloques rígidos embebidos en una matriz de suelo débil, donde la relación de rigidez entre ambos materiales es mayor a dos. La investigación en bimsoils se concentra en la determinación de los parámetros de resistencia en función de la proporción volumétrica de bloques (VBP). Sin embargo, la resistencia de bimsoils depende de otras variables, entre ellas el tamaño de los bloques. Aunque algunos autores indican que este no influye la resistencia, otros concluyen que la resistencia es mayor cuando la distribución de tamaños es bien gradada y el tamaño máximo del bloque es mayor. Este estudio presenta un análisis numérico de la influencia del tamaño del bloque y la VBP en los parámetros de resistencia de bimsoils, a partir de ensayos triaxiales drenados modelados en FEM. El tamaño de bloque es constante en todo el espécimen y corresponde a una fracción del diámetro de la muestra (D) que varía de 0.1 a 0.2. Se observa una mayor resistencia al corte en los bimsoils con valores elevados de VBP y tamaño de bloques entre $0.12D$ y $0.15D$. Esto se refleja en los parámetros de resistencia. La influencia del tamaño se observa para distintas VBP y cuando los bloques tienen una distribución espacial uniforme y columnar. El aumento de la VBP genera el incremento en la anisotropía de la magnitud de los esfuerzos principales en la muestra y los tamaños de bloques $0.12D$ y $0.15D$ generan una mayor heterogeneidad de los esfuerzos de corte reflejado en la magnitud y propagación de los esfuerzos en la muestra.

Palabras clave: bimsoils, tamaño de bloques, ensayo triaxial drenado, elementos finitos, proporción volumétrica de bloques

Introduction

Medley (1994) suggested using the term “bimrock”, coined by Raymond (1984) and derived from the geological concept of blocks within a rocky matrix or mixtures of rocks made up of rigid blocks within a fine matrix, to describe mixtures of relatively large, geotechnically significant competent blocks within a bonded matrix of finer and weaker textures. These mixtures exhibit a mechanical contrast between blocks and matrix, where the geometry and proportion of the blocks influence the mass properties of the rock at the scales of engineering interest (Medley and Zekkos, 2011). Examples of bimrocks include thick pyroclastic rocks, melanges (rock masses composed of competent rock blocks of various sizes embedded in a weak clay matrix), fractured breccia and streamers, faulty rocks, and weathered and highly tectonized rocks Lindquist and Goodman (1994); Medley (2004); Medley and Goodman (1994). Kalender *et al.* (2014) introduced the term ‘bimsoil’ to describe complex mixtures that include rock blocks surrounded by a soil matrix, a condition similar to colluviums and erratic glacial deposits.

Research on bimrocks and bimsoils can be grouped into three main topics: in situ characterization, the uncertainty of the volumetric proportion blocks (Medley, 2002a; Ramos-Cañón *et al.*, 2020), and shear strength-stiffness properties. The aforementioned topics are interconnected, as the geotechnical properties depend on the distribution and geological characteristics of these in situ mixtures.

The strength and deformation properties of bimrocks / bimsoils depend on the Volumetric Block Proportion (VBP). In bimrocks with very weak block-matrix contacts, an increase in VBP generally results in a linear increase in the friction angle and an exponential decrease in cohesion (Lindquist and Goodman, 1994; Sonmez *et al.*, 2006). For volumetric proportions between 20 % and 25 %, it is observed that the cohesion decreases drastically, and the block-matrix interaction controls the strength. After 25 %, the shear strength is characterized by negligible cohesion (Coli *et al.*, 2011) and the interlocking of blocks predominates, forming more tortuous failure mechanisms (Kahraman and Alber, 2006; Kahraman *et al.*, 2008, 2010). For lower values of VBP , the change in shear strength mainly consists of the contribution of the mobilized friction angle and the loss of cohesion.

Regarding in-situ characterization, it has been concluded that the sampling scale of material mixtures can be defined based on a characteristic dimension (Medley and Lindquist, 1995; Medley and Zekkos, 2011). Medley and Lindquist (1995); Medley and Zekkos (2011) conducted an analysis of the block size distributions on maps and aerial photographs of San Francisco melanges, normalized with respect to a characteristic dimension (L_c). In that case, it corresponded to the square root of the mapped area. The characteristic dimension can be any engineering measure, such as the width of a foundation, the height of a slope, or the diameter of a laboratory sample (D) and the distribution of the sizes of a bimrock must range between $0.05 L_c$ and $0.75 L_c$ (Medley and Lindquist, 1995). The scalability of the bimrocks sampling supports the assertion that laboratory samples can serve as representative models of in-situ masses because they are independent of the scale of interest.

On the other hand, the contribution of the VBP on the bimsoils strength is reflected mainly in the increase in the mobilized friction angle defined as the sum of the critical friction (φ_c) and dilation components (ψ) (Gong and Liu, 2015; Holtz, 1960; Irfan and Tang, 1993; Patwardhan *et al.*, 1970). Irfan and Tang (1993) concluded that VBP does not have a well-defined influence on cohesion, while Miller and Sowers (1958) noted that cohesion increases for low VBP (higher proportion of matrix) due to the generation of compaction areas in the matrix located between blocks.

Research on the size of blocks in bimrocks primarily focuses on in-site characterization Coli *et al.* (2009); Medley (2002b); Medley and Zekkos (2011). In-situ characterization aims to estimate the distribution of block sizes in melanges and mixtures of shales and silt through photographic analysis. Medley and Zekkos (2011) indicated that the sizes of the blocks follow a potential distribution, with the exponent corresponding to the fractal dimension obtained from the analysis of various photographs.

Most of the experimental studies have focused on the influence of VBP , block distribution, and orientation on the shear strength of bimsoils. A variety of test methods have been employed, including in-situ tests (Chu *et al.*, 1996; Coli *et al.*, 2011; Gao *et al.*, 2021; Liang *et al.*, 2023; Wen-Jie *et al.*, 2011; Zhang *et al.*, 2016b), small- and large-scale monotonic triaxial tests (Chu *et al.*, 2010; Jin *et al.*, 2017; Lindquist and Goodman, 1994; Wang *et al.*, 2018; Zhang *et al.*, 2016a), cyclic triaxial tests (Cao *et al.*, 2017; Wang *et al.*, 2021), monotonic direct shear tests (Avşar, 2021; Cen *et al.*, 2017; Hu *et al.*, 2024), and cyclic torsional simple shear tests (Ishikawa and Miura, 2015). Note that uniaxial compression tests (Afifipour and Moarefvand, 2014; Avşar, 2020; Mahdevari and Moarefvand, 2018) were only performed for bimrocks (welded materials), as additional cementing agents were required.

Numerical and experimental research on the specific influence of block size on bimsoils is limited. Holtz and Gibbs (1956) concluded that the size of the blocks does not influence the shear strength of the gravel and sand mixtures, while Donaghe and Torrey (1979); Rathee (1981) indicated that the shear strength of bimsoils with well-graded size distributions is higher when the maximum size of the blocks is large. For bimsoils with a predominantly granular matrix, the increase in shear strength is reflected in the friction angle, so the increase in the maximum block size generates an increase in the mobilized friction angle (Rathee, 1981). Sheikhpourkhani *et al.* (2024) produced DEM modeling results showing that an increase in volumetric block proportion (VBP) reduces uniaxial compressive strength (UCS) and cohesion, but increases the internal friction angle due to the occlusion effect of the blocks. The study highlights that block-matrix contacts dominate the failure mechanism up to a VBP of 40 %, while block-block contacts become more significant at higher VBP values. Sharafisafa *et al.* (2024) numerically investigated the impact of the strain rate on the failure mechanisms of bimrocks with varying volumetric block proportions (VBP). Different strain rates were applied to specimens with VBP s between 25 % to 90 %. Results revealed that strain rate significantly affects failure patterns, peak stress, and post-peak behavior. At low to medium strain rates ($\leq 0.18/s$), failure patterns are consistent, while higher rates induce complex failure modes such as multiple fracturing and axial splitting, with a rapid peak stress increase. Bimrocks with VBP s up to 75 % exhibit similar strain rate sensitivity, whereas specimens with 90 % VBP show minimal variation in failure type (primarily axial splitting) and peak stress.

Due to the discrepancies in prior interpretations and limited investigations regarding the effect of block size on bimsoil strength, this study focuses on examining the influence of block size at low VBP on the variation of the cohesion and friction angle. Notably, the variation of the cohesion is associated with the generation of compaction areas at low VBP s.

The influence of spherical block size on the shear strength parameters of bimsoils with low ($VBP < 30\%$) is quantified by means of finite element models. To isolate the effects of block size and VBP , 3D models of triaxial tests with different VBP were performed in the finite element software ABAQUS using the Mohr-Coulomb constitutive model, for cylindrical specimens with 10 cm in diameter and 10 cm in height (1:1 ratio), where the blocks are spherical. The size of blocks does not change in a specimen, and the random spatial location follows a uniform distribution.

The results indicate that the strength parameters increase with both increment of VBP and with block size up to a range corresponding to 12 % and 15 % of the diameter of the sample (D) and then it decreases to the same value that was obtained with the smallest size (10 % D). The soils with $0.12D$ and $0.15D$ blocks show a greater magnitude and distribution of the shear stresses in the entire sample.

Materials properties (blocks and matrix)

Bimsoil are made up of rigid blocks and a weak soil matrix, so the definition of the properties is presented for each component separately.

Blocks

The properties of a granitic rock are used to characterize the rigid spherical blocks. A linear elastic constitutive model was selected, as no plastic deformation is expected under the stress conditions applied to the bimsoil sample in the numerical simulations. The model parameters for the blocks were obtained considering the properties of the granite. [Zhang \(2016\)](#) presents that the modulus of elasticity (E) and the Poisson ratio (ν) of granite vary between 6 - 100 GPa and 0.09 - 0.39, respectively. For the ABAQUS model, the elastic parameters $E = 52$ GPa and $\nu = 0.19$ were selected.

Matrix

The weak matrix is represented by a light overconsolidated soft clay, modeled using the Mohr-Coulomb constitutive model available in ABAQUS. An element test simulation based on the finite element model with one element was generated to reproduce the softening behavior expected for lightly overconsolidated clay soils. This simulation replicated the triaxial test conditions with volumetric change. The parameters were calibrated until a good match was obtained with experimental results of overconsolidated kaolin reported by [Sachan and Penu-madu \(2007\)](#).

The Mohr-Coulomb constitutive model available in ABAQUS requires defining the following parameters: elasticity modulus (E), the Poisson ratio (ν), friction angle (φ), dilation angle (ψ), cohesion (c), and the equivalent plastic deformation (ε_{eq}^p). The parameter ε_{eq}^p is very sensitive and, together with the cohesion, controls the softening shape for the stress-strain curve. The values presented in Table 1 were determined through calibration using the experimental data reported by [Sachan and Penumadu \(2007\)](#). Figure 1 shows the simulation of the element test and the laboratory deviatoric stress ($\sigma_1 - \sigma_3$) vs axial strain (ε_1). The relative differences in peak stress ($\Delta\sigma_p$), strain at peak stress ($\Delta\varepsilon$) and residual stress ($\Delta\sigma_r$) are small.

Tabla 1. Parameters used for kaolin ([Sachan and Penumadu, 2007](#)) and clay matrix

Parameter	Kaolin (Sachan and Penumadu, 2007)	Clayey matrix
E	2500 kPa	10000 kPa
ν	0.32	0.32
φ	12°	12°
ψ	0.1°	3°
c	18 kPa - 18 kPa - 6 kPa	30 kPa - 30 kPa - 10 kPa
ε_{eq}^p	0 - 0.15 - 0.6	0 - 0.15 - 0.6

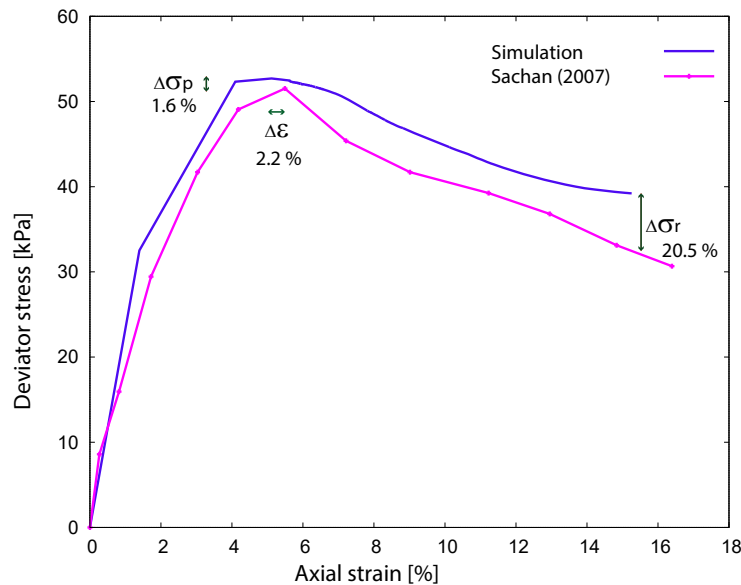


Figura 1. Differences of the deviator stress - axial strain curves of the simulation and kaolin reported by ([Sachan and Penumadu, 2007](#))

Numerical model

A 3D finite element model of a cylindrical specimen subjected to confining stresses of 75 kPa, 150 kPa, and 300 kPa was created in ABAQUS. A controlled vertical displacement equivalent to an axial deformation of 20 % was subsequently prescribed. Given that the mechanical behavior of a bimsoil depends on numerous variables—and the aim of this study is to investigate the influence of the size of the blocks and the *VBP* on the shear strength—the problem was specified as follows:

- The cylindrical sample has a diameter and height of 10 cm (1:1 ratio), ensuring that the geometry does not favor any particular direction for block distribution. This prevents the specimen's shape from influencing the test response with a variable deformation-stress behavior due to the heterogeneity of the soil (Lade and Wasif, 1988).
- The blocks are spherical in shape and randomly distributed within the sample following a uniform distribution.
- The *VBP* is low (15 %, 20 % and 25 %) and represents the zone in which bimsoils reflect an exponential decrease in cohesion (Sonmez *et al.*, 2006). This reduction is attributed to an increase in soft compaction areas between the blocks (Miller and Sowers, 1958).
- Block sizes range from $0.05 D$ to $0.75 D$, where D represents the characteristic dimension—specifically, the diameter of the cylindrical specimen (Medley and Lindquist, 1995). Five block sizes (10 mm, 12 mm, 15 mm, 18 mm and 20 mm) were defined with a mono-disperse distribution in the entire sample and are represented as a fraction of the diameter of the sample (D).
- Blocks and surrounding matrix are linked together and cannot move independently from each other.
- A triaxial test model with volume change was simulated using ABAQUS. The boundary conditions of a triaxial specimen were reproduced with the placement of two rigid steel plates, in the upper and lower area of the sample representing the triaxial cap and pedestal. The lower plate remains fixed and the upper plate is subjected to a vertical displacement of 2 cm corresponding to 20 % axial strain calculated with the initial height of the specimen.

The numerical model is generated from the definition of the geometry, loads, contour, and mesh conditions. The geometry consists of independently generating the blocks and the clay matrix to later assemble it in finite element software. Loads and boundary conditions obey the imposition of the confining stress and then, the vertical displacement of 20 mm was applied.

Geometry

A procedure was implemented in MATLAB to randomly generate the coordinates x , y , and z of the center of each block. These coordinates were required to follow a uniform distribution function throughout the sample. The ratio of the volume of all the spheres and the volume of the sample corresponds to the defined VBP . The spheres must be fully embedded in the sample and cannot overlap each other. Since the characteristic dimension in the finite element model corresponds to the diameter of the sample (D), the block sizes are represented as a fraction of the diameter. Thus, 10 mm diameter blocks correspond to $0.1D$.

Loads and boundary conditions

To simulate the conditions of a drained triaxial test, the model includes an upper and a lower plate of the sample, defined as rigid bodies. The plates interact with the sample using ABAQUS contact elements `surface-surface`, a type restriction `penalty` and with a Coulomb isotropic friction model. The parameter of this contact model is the coefficient of friction between surfaces (μ), which was defined as 0.15 for the contact of a cohesive material and steel. This coefficient relates the tangential stress to contact pressure. Slip occurs if during the simulation the equivalent tangential stress (magnitude of all tangential stresses) exceeds the critical stress (defined by μ) (Hibbitt *et al.*, 2001).

The loads and boundary conditions were defined in three sequential steps. First, an initial stage involved the imposition of the contact model, during which both the upper and lower plates remained fixed. Second, a confinement stage was implemented by applying pressure around the specimen and at a reference point located at the center of the upper plate, aligned with the axis of the sample. Finally, a shear stage was executed through controlled vertical displacement of the upper plate, reaching 20 % axial strain relative to the initial height of the specimen. Figure 2 shows the ABAQUS model, with all the imposed loads and boundary conditions.

Mesh

The model meshing is important because numerical results depend on the element type and refinement of the mesh. Given the cylindrical and spherical features of the model geometry, a free meshing technique is employed, as recommended in ABAQUS. This technique uses tetrahedral elements with linear approximation (C3D4). The choice of linear elements was motivated by computational efficiency: linear approximation significantly reduces processing time compared to a quadratic approximation. Considering the total number of models generated is 45 (3 VBP , 5 block sizes and 3 confining pressures); the linear approximation was

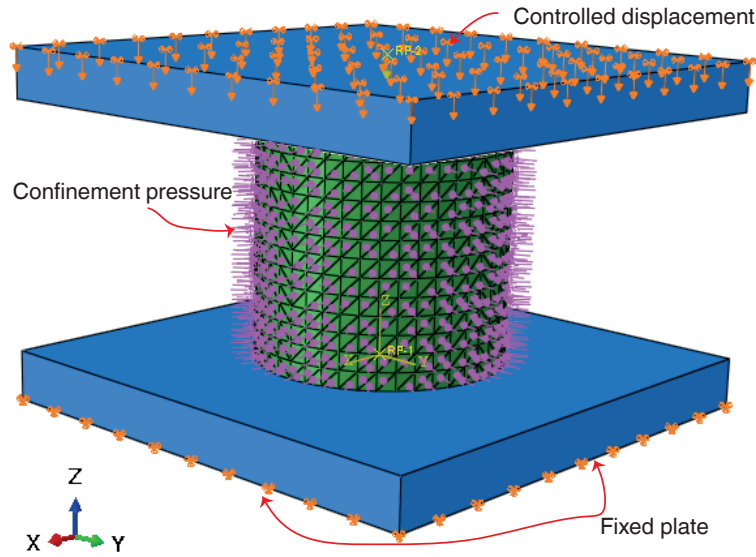


Figura 2. Loads and boundary conditions in the sample

deemed optimal for reducing computational cost.

Mesh refinement was achieved through the use of partitions in the geometry, conditions in the number of nodes located at the edges of the geometry (seeds), and the definition of the edge distance of element (s). A series of tests were carried out with different values of s until a value of $s = 0.007$ was selected, which is the maximum value that the edges of the element can take so that the results of deformation stress curves present the least mean square error (MSE) as can be seen in Figure 3.

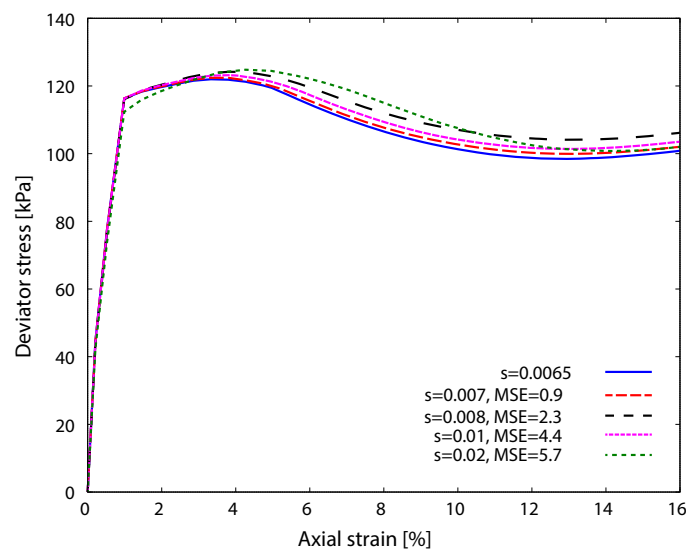


Figura 3. Strain-stress curves for matrix samples with confinement of 150 kPa and different values of edge distance of element parameter s

Tabla 2. Mesh verification criteria (Hibbitt *et al.*, 2001)

Criteria	Value for tetrahedron
Form factor	0.0001
Minimum angle	5°
Maximum angle	170°
Aspect ratio	10
Geometric deviation factor	0.2

The meshes for the matrix and blocks were generated separately. Material properties were assigned to the elements of each mesh and then joined to form an assembly in ABAQUS. In this model, mesh-based fixed bonding implies that any movement imposed on a block results in a corresponding movement of the surrounding clay matrix, without separation—thus representing a welded condition.

In addition, the mesh verification was performed to assess the quality of the generated elements. This process involved evaluating the form factor, the maximum and minimum angles between nodes, the aspect ratio, and the geometric deviation factor of the elements comprising the model. Table 2 shows the limits of each of the verification measures mentioned. The statistics of the models show that only the bimsoil with *VBP* of 15 % and block size 10 mm had a tiny fraction of 0.00557 % of elements that do not comply with what is specified in the Table 2.

Effect of *VBP* on the shear strength of bimsoil

The 45 numerical triaxial tests with volume change (5 block sizes and 3 *VBP*), simulated in this work under the conditions indicated in the previous section, demonstrate that shear strength interpreted with the Mohr-Coulomb strength criterion increases with the *VBP*. This is reflected in both the mobilized friction angle and cohesion. One way to visualize this trend is through the distribution of shear stresses, represented in ABAQUS by the von Mises stress invariant, developed in the sample, where the most rigid component (the blocks) has a higher stress concentration than the weak matrix. Figure 4 shows that at the same level of axial strain (10 %), when the *VBP* increases, there are larger shear stresses that create “bridges” between the blocks, considering that the location of the blocks is uniform throughout the sample. These transmissions of shear stresses are represented with red links in Figure 4, and it is evident that the higher *VBP*, the more linked blocks.

Plots of deviator stress ($\sigma_1 - \sigma_3$) versus axial strain (ε_1) for all bimsoils show a hardening behavior. From 3 % of axial strain onward, a noticeable difference emerges between the strength

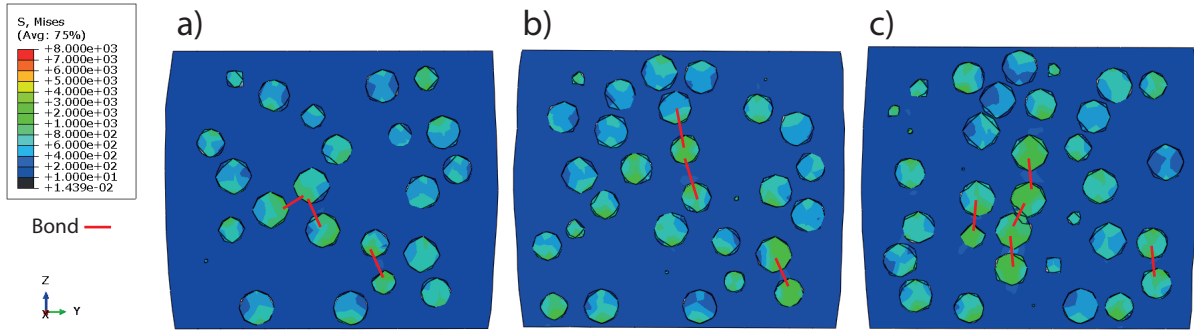


Figure 4. Von Mises stress distribution at 10 % deformation in bimsoils samples for a block size of 0.12 D and VBP of a) 15 %, b) 20 % and c) 25 %

of bimsoil samples and that of samples composed of solely matrix material (see Figure 5) for different VBP . The strain hardening behavior resembles the mechanical response of a colluvial deposit that, as it slides, resists more until it mobilizes all its strength and stops (Irfan and Tang, 1993). On the other hand, Barton (2013) argues that the shear strength of a saprolite presents hardening in the zone of influence of clay, followed by a significant strength increase in the zone of influence of the blocks (high deformations).

At the onset of the shear ($\varepsilon = 0\%$), the direction of principal stress, obtained from the nodes of the entire specimen, presents a uniform distribution of frequencies quantified with a K-S test at 95 % reliability, and it was found that after 3 % axial deformation, anisotropy begins to appear in the directions of the principal stresses. The anisotropy of the directions of the principal stresses of the sample, determined according to the nomenclature of the continuum mechanics (tension positive, compression negative), begins at 3 % axial deformation at which strength differences first appear between the specimens with only matrix and the specimens with blocks. The anisotropy of the principal stress directions is presented in Figure 6, which shows the accumulated frequencies of the angles formed between the minor principal stress (σ_3) and the direction of application of the controlled displacement (axis z) across all the nodes of the sample. As axial deformation increases, the anisotropy in stress direction progressively vanishes, regardless of block size or VBP . This trend was observed in all the tested bimsoils triaxial specimens.

On the other hand, the ratio of intermediate principal stresses (b), defined by Eq. 1 (see Figure 7). When b is close to 1, there is an orthotropic stress state, as observed in the matrix case. As b decreases, the stress state is more anisotropic, as with bimsoils. The values of b are obtained from the principal stresses of the nodes of the entire sample at a deformation level of 10 % and are grouped to define their distribution. The accumulated frequencies of b for the

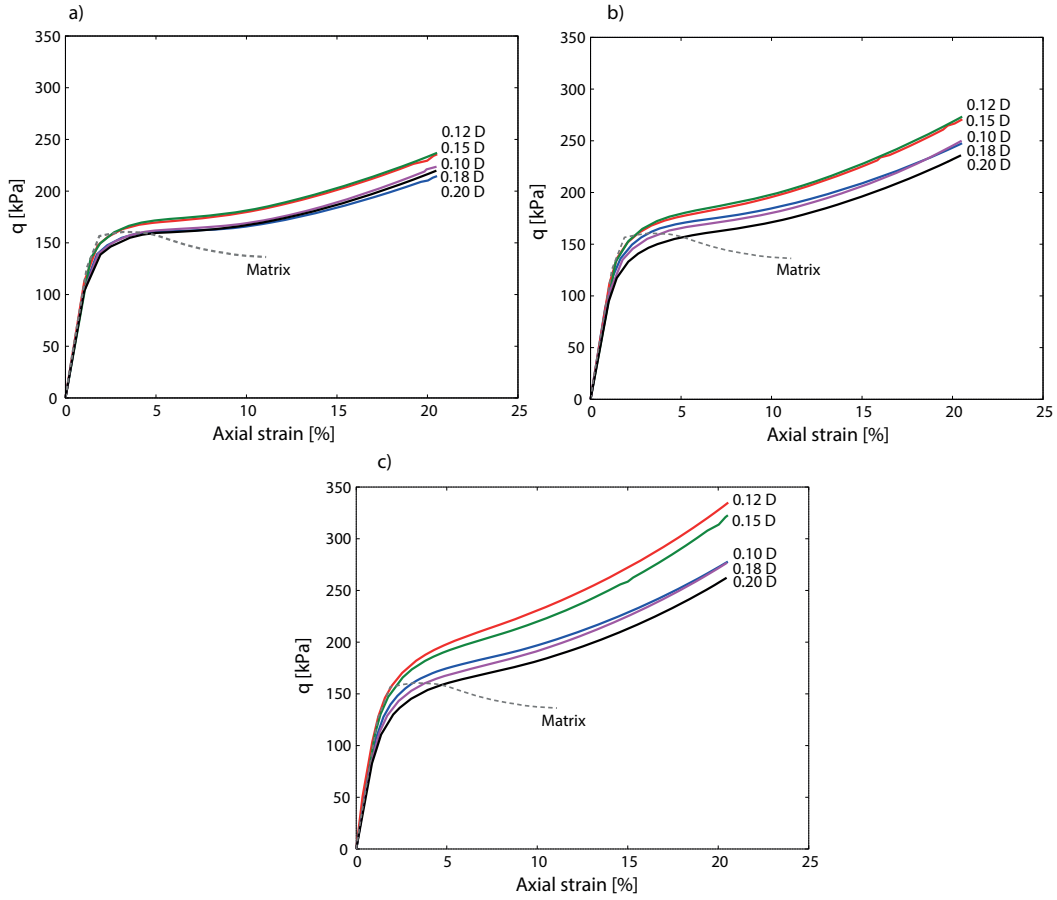


Figure 5. Deviator stress - axial strain curves for *VBP* of a) 15 %, b) 20 % and c) 25 %.

matrix and bimsoils indicate that a *VBP* of 25 % corresponds to a median of 0.73, while a *VBP* of 15 % has a median of 0.79. These results confirm that higher *VBP* levels induce greater anisotropy in the magnitude of the main stresses within the samples.

$$b = \frac{\sigma_2 - \sigma_3}{\sigma_1 - \sigma_3} \quad (1)$$

Since the simulated bimsoil exhibits strain-hardening behavior, the Lambe (MIT) triaxial stress invariants s' (centre of Mohr's circle) and t (radius of Mohr's circle) were calculated at different deformation levels to obtain the mobilized friction angle and cohesion. Results indicate that cohesion tends to decrease while the mobilized friction angle increases with axial strain, regardless of *VBP* and block size (see Figure 8).

For bimsoils with low *VBP*, the increase in the friction angle is primarily attributed to the volumetric dilation—i.e., the increase in volumetric strain relative to axial strain—since in these cases, no significant friction or contact between blocks was observed. In contrast, when the *VBP* is greater than 25 %, the behavior of bimsoils is dominated by friction and dilation, while

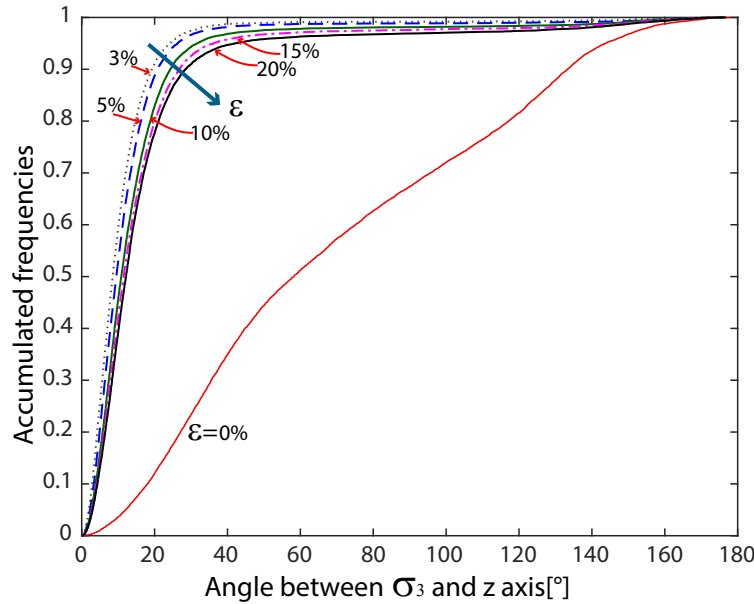


Figura 6. Variation of the accumulated frequencies of the angle between the minor principal stress σ_3 and the vertical axis z with the axial deformation in bimsoils samples with VBP of 25 % and block size $0.12 D$.

the contribution from cohesion—originating from the clay matrix between blocks—diminishes (Iannacchione and Vallejo, 2000).

Figure 8 shows that the mobilized strength envelope for different strain levels follows a linear trend. For confining stress levels exceeding 500 kPa, it could be expected that the strength envelope of a geomaterial would exhibit a curvilinear behavior, suggesting that a linear Mohr-Coulomb strength model with respect to the confinement stress would not be the most suitable to represent this behavior. However, this is not the case for the numerical results presented in Figure 8, as the stress confinement levels used in the triaxial simulations were 75 kPa, 150 kPa, and 300 kPa.

Effect of blocks size on the strength of bimsoils

The present study focuses on bimsoils composed of uniformly sized blocks throughout the specimen, allowing for the isolated analysis block size and VBP , without considering the effect size gradation. The size of the blocks does indeed influence the strength of bimsoils and the one that provides the greatest strength is the range from $0.12D$ to $0.15D$ for the three VBP used. Figure 5 shows the deviator stress - axial strain curves of bimsoils for different VBP s.

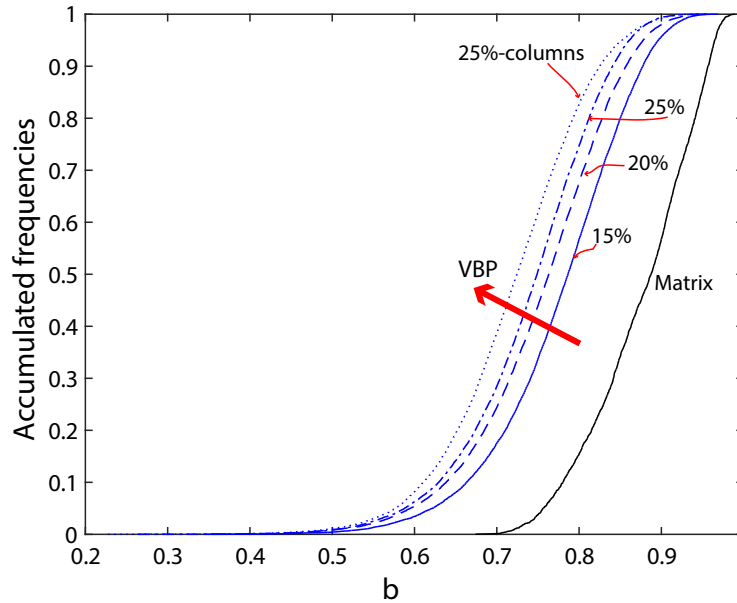


Figura 7. Cumulative frequencies of the ratio of intermediate principal stresses b in bimsoils samples for a block size $0.12D$ at 10% deformation.

In the same way, the mobilized friction angle and cohesion are greater for bimsoils with blocks of size $0.12D$ and $0.15D$, as seen in Figures 9 and 10 for different levels of axial deformation. The variation of the mobilized friction angle and cohesion, normalized with respect to the friction angle and cohesion of the matrix, has been represented on three-dimensional surfaces where the independent axes are the variable VBP and the block size normalized by the diameter of the sample. Both parameters increase with the VBP , and with respect to block size, they increase up to the $0.12D$ to $0.15D$ range before decreasing. This shape of the surfaces indicates that there is a direct relationship between the size $0.12D$ and the magnitude and transfer of stresses that are generated in the sample. This is illustrated in Figure 11, where the sample with blocks $0.12D$ presents more zones with stresses greater than 350 kPa.

When analyzing shear stresses greater than 350 kPa generated in the nodes of the sample, it was observed that for a VBP of 25%, both the mean and the coefficient of variation of the shear stresses are greater for the block size $0.12D$. As shown in Figure 11, a greater number of high-stress zones (above 350 kPa) are distributed throughout the sample for this configuration. The cumulative frequencies of the Von Mises invariant of the sample nodes, defined by Eq. 2 where S denotes the full tensorial deviatoric stress, indicate that the range of stresses increases with axial deformation. By comparing stresses at 75% (quartile 3) and 25% (quartile 1) of these distributions, significant differences emerge among bimsoils with varying block sizes. To quantify this variation, the Heterogeneity Index was defined ($HI = \sigma_{75\%}/\sigma_{25\%}$). This in-

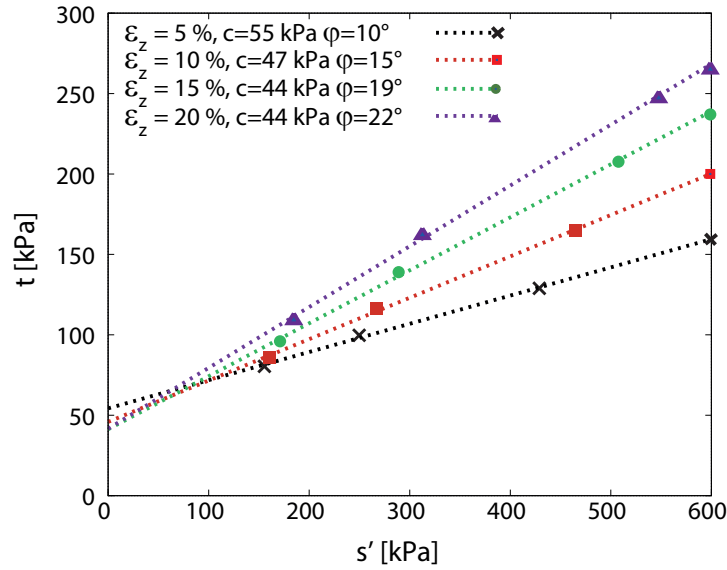


Figura 8. Mobilised friction angle and cohesion for different levels of axial deformation of a Bimsoil with *VBP* of 25 % and blocks size of $0.12D$.

dex provides a measure of stress distribution within the sample: higher values of *HI* indicate a more heterogeneous distribution of shear stresses and correspond to higher coefficients of variation.

$$q = \sqrt{\frac{3}{2}(\mathbf{S} : \mathbf{S})} \quad \text{with} \quad \mathbf{S} = \boldsymbol{\sigma} - \frac{1}{3}\text{tr}(\boldsymbol{\sigma})\delta_{ij} \quad (2)$$

The *HI* of all samples at different strain levels is higher for samples with block size $0.12D$. This indicates a direct relationship between size $0.12D$ and the heterogeneity of the efforts it generates. Figure 12 shows the variation of the Heterogeneity Index with size and *VBP* for an axial strain level of 10 %. For *VBP* of 25 %, the average Von Mises stresses and the size $0.12D$

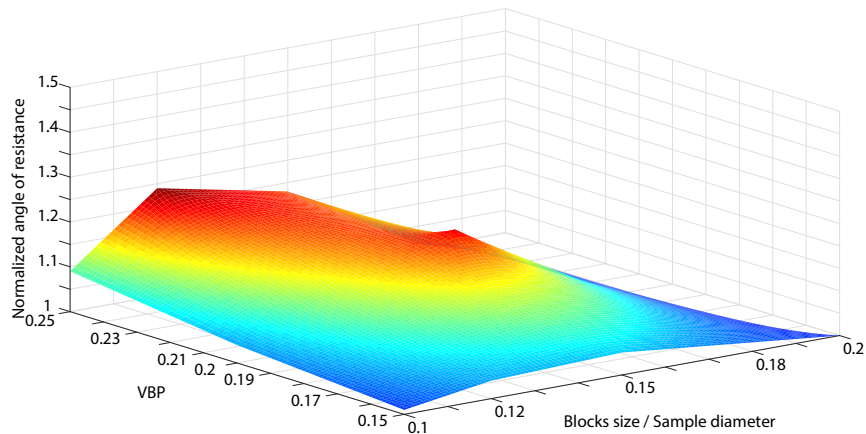


Figura 9. Variation of the mobilized friction angle depending on the size and *VBP* at 10 % deformation.

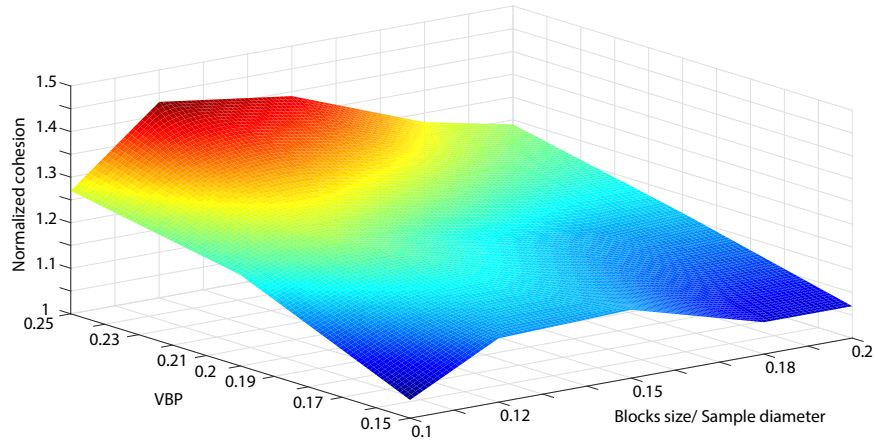


Figura 10. Variation of the cohesion depending on the size and *VBP* at 10 % deformation.

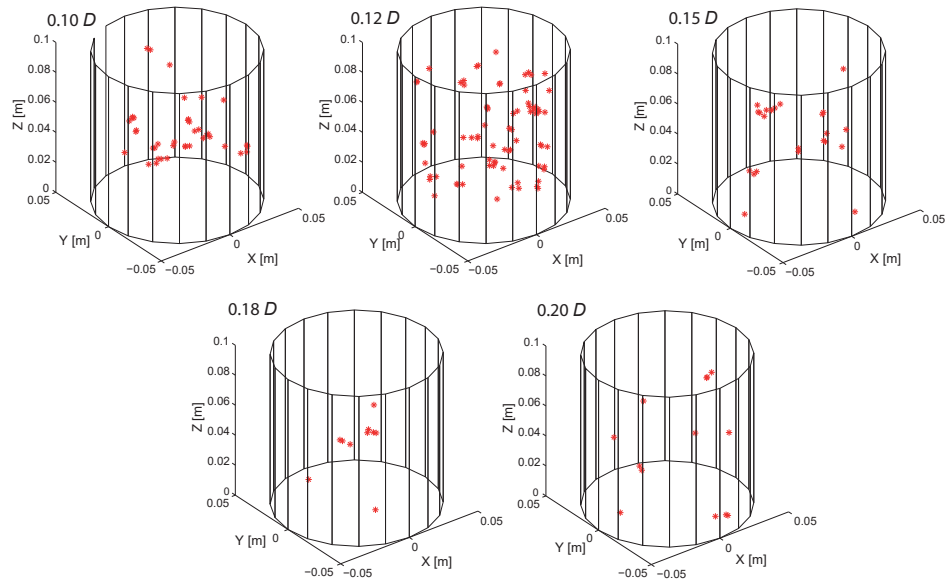


Figura 11. Shear stresses greater than 350 kPa in bimsoils samples with *VBP* of 25 %.

exhibit a higher average shear stresses and *HI*, leading to the conclusion that this block size generates a greater shear stress magnitude and a more heterogeneous stress distribution within the sample. Furthermore, when increasing the *VBP* the block size of $0.2D$ generates a heterogeneity index greater than the block size $0.18D$, which is also reflected in the surfaces of the Figure 9.

The block size does not influence the orientation of the principal stress directions within the sample, as all the samples at the same *VBP* show no variation in the cumulative probability distribution curves. Hence, the size only influences the magnitude and distribution of the shear stresses.

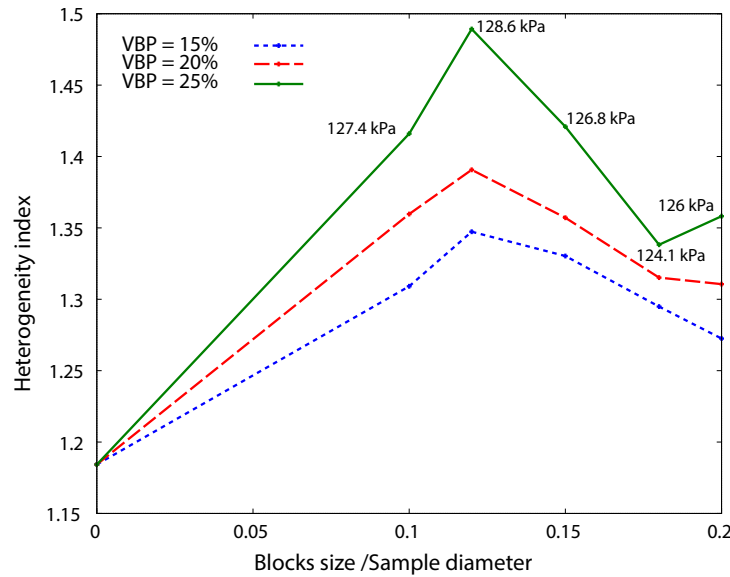


Figura 12. Variation of the heterogeneity index with blocks size and VBP .

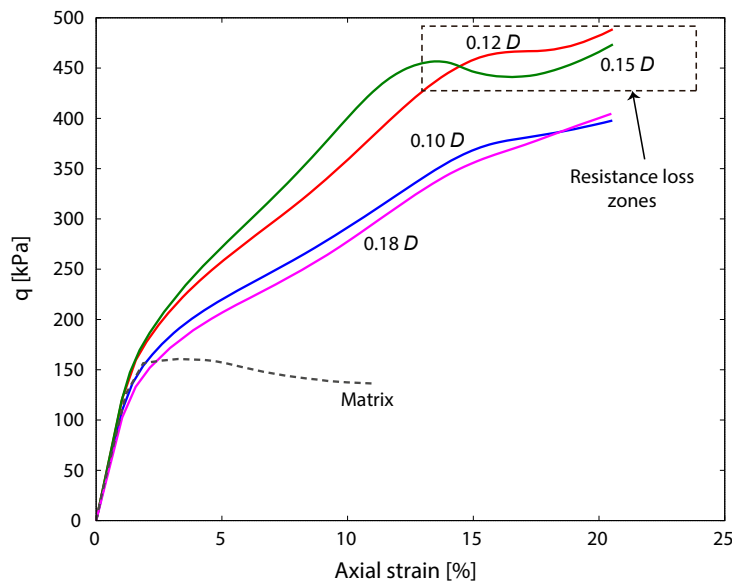


Figura 13. Axial strain-stress curves in bimsoils with $VBP = 25\%$ and columns spatial distribution.

By varying the location of blocks from a uniform random array to a columnar configuration without changing VBP , the effect of block size $0.12D$ is maintained. Triaxial simulations were conducted on bimsoils with a VBP of 25 % and different sizes, with the blocks positioned vertically one above the other to form columns. The results of the models indicate that the strength of bimsoils with a columnar location is twice that of the uniform location and that block sizes $0.12D$ and $0.15D$ develop greater strength than the other sizes. This new spatial distribution of

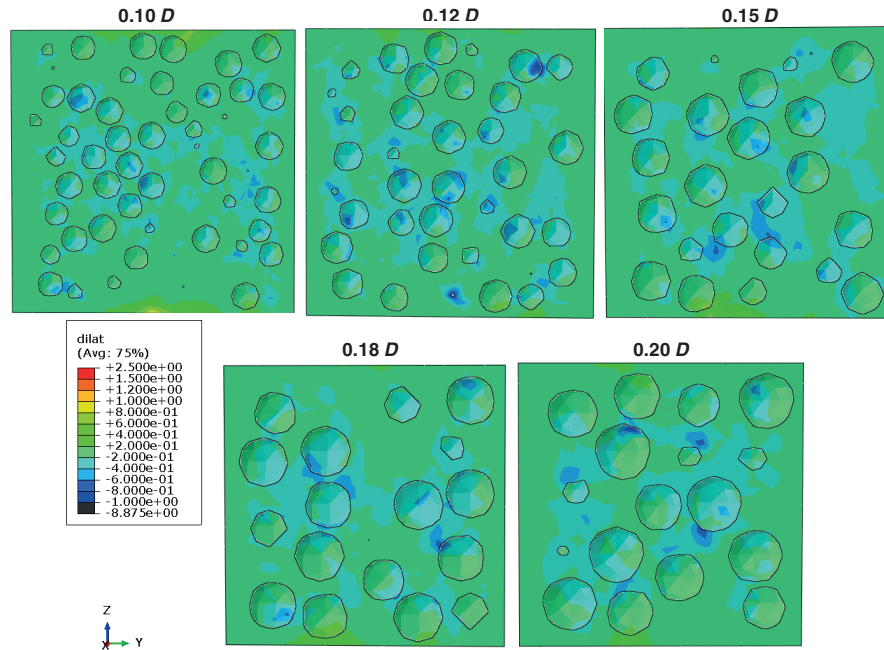


Figure 14. Compaction areas for bimsoils samples with VBP of 25 %.

the blocks greatly affects the shear strength and generates areas of loss of strength when the blocks break the configuration of columns (strain greater than 10 %) and regain strength when nearby blocks support their new position (see Figure 13).

As previously described by [Irfan and Tang \(1993\)](#) and [Medley and Rehmann \(2004\)](#), block location is a variable that influences the magnitude of the stresses and the anisotropy of the stress state. The bimsoil sample with VBP of 25 % and columnar block arrangement (independent of block size) greater stress anisotropy is observed. This is reflected in a lower value of b , compared to bimsoils with the same VBP , but uniform location (see Figure 7).

In all cases, sizes $0.12D$ and $0.15D$ result in greater shear strength, as reflected in the mobilized friction and cohesion. The increase in mobilized friction angle is attributed to global dilation, measured at the nodes of the sample periphery. The higher cohesion is due to the formation of compaction areas in the matrix located between blocks, measured in the nodes and exhibiting the greatest deformation. This aligns with the findings of [Miller and Sowers \(1958\)](#) who analyzed the influence of VBP in experimental laboratory tests. Figure 14 shows the mapping of the compaction areas obtained from dilation values at all sample nodes. Dilation is represented by the positive sign and contraction by the negative sign. The presence and concentration of compaction areas (blue contours) in the samples with blocks of size $0.12D$ and $0.15D$ is greater than in the other samples.

Conclusions

Numerical simulations in ABAQUS of triaxial compression tests on mixtures of rigid blocks embedded in a fine matrix revealed that shear strength increases with rising *VBP* when the axial strain exceeds 3 %. This trend is evident in the Mohr-Coulomb shear strength parameters—specifically, the friction angle and cohesion. At this level of axial strain, anisotropy in the directions of the principal stresses begins to develop within the samples. As a result, the contribution of rigid blocks to large deformations becomes significant, as observed by Barton [Barton \(2013\)](#). The *VBP* influences the stress state; when it increases the anisotropy in the magnitude of the principal stresses—defined by the relation of intermediate stresses *b*—also increases.

For all *VBP*s, the bimsoils shear strength increases with increasing size, up to a threshold between 12 % and 15 % of the sample diameter. These block sizes allow for geometric configurations that generate a greater quantity and magnitude of Von Mises deviatoric stresses at the nodes, making the samples more heterogeneous compared to those with other block sizes.

The heterogeneity of the shear stresses in the sample was quantified using a proposed Heterogeneity Index *HI*, defined as the relationship between quartile 3 and quartile 1 of shear stress values. A higher *HI* indicates more extensive branching of stresses throughout the sample. The highest *HI* was observed in samples with blocks of size $0.12D$, no matter the *VBP*. For a *VBP* of 25 %, shear stresses developed are 45 % greater than the stresses in samples with other block sizes (see Figure 12).

Block location within the specimens is an important variable in bimsoils shear strength. For the same *VBP* and any block size, the samples with blocks forming columns generate twice the magnitude of shear strength and higher anisotropy of the stress state than the samples with blocks located uniformly. This behavior is explained because the location in columns facilitates the immediate transmission of stresses.

The angle of friction has a predominantly dilating component and is higher for sizes of $0.12D$ and $0.15D$, due to greater global dilation, which was measured at the nodes located on the periphery of the sample.

Similarly, cohesion is higher for sizes of $0.12D$ and $0.15D$, resulting from the formation and concentration of compaction zones within the matrix between blocks (see Figure 14). These compaction areas aligned with the theory proposed by [Miller and Sowers \(1958\)](#), based on an experimental investigation of bimsoils with clayey matrices, as further discussed by [Iannacchione and Vallejo \(2000\)](#).

The mobilized strength envelope for different strain levels and VBP values is linear in the MIT-Lambe triaxial stress invariants space. This behavior can be attributed to the moderate employed in the present simulations. It is expected that, under higher confinement stress levels, the strength envelope would exhibit nonlinear behavior. Likewise, further analysis using very low confinement stresses could help determine whether the nonlinearity observed in experimental studies of other geomaterials also applies to bimsoils.

References

- Afifipour, M. and Moarefvand, P. (2014). Mechanical behavior of bimrocks having high rock block proportion. *International Journal of Rock Mechanics and Mining Sciences*, 65:40–48. ↑ 33
- Avşar, E. (2020). Contribution of fractal dimension theory into the uniaxial compressive strength prediction of a volcanic welded bimrock. *Bull. Eng. Geol. and the Envir.*, 79(7):3605–3619. ↑ 33
- Avşar, E. (2021). An experimental investigation of shear strength behavior of a welded bimrock by meso-scale direct shear tests. *Eng. Geology*, 294:106321. ↑ 33
- Barton, N. (2013). Shear strength criteria for rock, rock joints, rockfill and rock masses: Problems and some solutions. *Journal of Rock Mechanics and Geotechnical Engineering*, 5(4):249–261. ↑ 40, 48
- Cao, Z., Chen, J., Cai, Y., Gu, C., and Wang, J. (2017). Effects of moisture content on the cyclic behavior of crushed tuff aggregates by large-scale tri-axial test. *Soil Dyn. Earthqu. Eng.*, 95:1–8. ↑ 33
- Cen, D., Huang, D., and Ren, F. (2017). Shear deformation and strength of the interphase between the soil–rock mixture and the benched bedrock slope surface. *Acta Geotech.*, 12:391–413. ↑ 33
- Chu, B., Pan, J., and Chang, K. (1996). Field geotechnical engineering properties of gravel formations in western taiwan. *Sino-Geotechnics*, 55:47–58. ↑ 33
- Chu, B.-L., Jou, Y.-W., and Weng, M.-C. (2010). A constitutive model for gravelly soils considering shear-induced volumetric deformation. *Can. Geotech. J.*, 47(6):662–673. ↑ 33
- Coli, N., Berry, P., and Boldini, D. (2011). In situ non-conventional shear tests for the mechanical characterisation of a bimrock. *International Journal of Rock Mechanics and Mining Sciences*, 48(1):95–102. ↑ 32, 33

- Coli, N., Berry, P., Boldini, D., and Bruno, R. (2009). Investigation of block geometrical properties of the shale-limestone chaotic complex bimrock of the santa barbara open pit mine (italy). In *Rock Engineering in Difficult Conditions, 3rd Canada-US Rock Mechanics Symposium, Toronto (CA)*, pages 9–14. ↑ 32
- Donaghe, R. and Torrey, V. (1979). Scalping and replacement effects on strength parameters of earth-rock mixtures. In *Proc. Conf. on Design Parameters in Geotechnical Engineering*, volume 2, pages 29–34. ↑ 33
- Gao, W., Iqbal, J., and Hu, R. (2021). Investigation of geomechanical characterization and size effect of soil-rock mixture: a case study. *Bull. Eng. Geol. and the Envir.*, 80(8):6263–6274. ↑ 33
- Gong, J. and Liu, J. (2015). Analysis on the mechanical behaviors of soil-rock mixtures using discrete element method. *Procedia Engineering*, 102:1783–1792. ↑ 32
- Hibbitt, Karlsson, and Soreson (2001). *ABAQUS/Standard User's Manual*. Hibbit, Karlsson & Sorensen, Inc., United States (Pawtucket). ↑ 37, 39
- Holtz, W. (1960). Discussion of testing equipment, techniques and errors. In *Research Conference on Shear Strength of Cohesive Soils*, pages 997–1002. ASCE. ↑ 32
- Holtz, W. and Gibbs, H. J. (1956). Triaxial shear tests on pervious gravelly soils. *Journal of the Soil Mechanics and Foundations Division*, 82(1):1–22. ↑ 33
- Hu, Y., Sun, S., Sun, Y., Wei, J., Le, H., Li, K., and Zhao, B. (2024). An experimental investigation of the effects of block proportion on bimrocks, considering different block-to-matrix strength ratios. *Materials*, 17(5):1114. ↑ 33
- Iannacchione, A. T. and Vallejo, L. E. (2000). Shear strength evaluation of clay-rock mixtures. *Geotechnical Special Publication*, pages 209–223. ↑ 42, 48
- Irfan, T. and Tang, K. (1993). *Effect of the coarse fractions on the shear strength of colluvium*. Geotechnical Engineering Office, Civil Engineering Department. ↑ 32, 40, 47
- Ishikawa, T. and Miura, S. (2015). Influence of moving wheel loads on mechanical behavior of submerged granular roadbed. *Soils Found.*, 55(2):242–257. ↑ 33
- Jin, L., Zeng, Y., Xia, L., and Ye, Y. (2017). Experimental and numerical investigation of mechanical behaviors of cemented soil-rock mixture. *Geotechnical and Geological Engineering*, 35:337–354. ↑ 33
- Kahraman, S. and Alber, M. (2006). Estimating unconfined compressive strength and elastic modulus of a fault breccia mixture of weak blocks and strong matrix. *International journal of rock mechanics and mining sciences*, 43(8):1277–1287. ↑ 32

- Kahraman, S., Alber, M., Fener, M., and Gunaydin, O. (2008). Evaluating the geomechanical properties of misis fault breccia (turkey). *International Journal of Rock Mechanics and Mining Sciences*, 45(8):1469–1479. ↑ 32
- Kahraman, S., Alber, M., Fener, M., and Gunaydin, O. (2010). The usability of cerchar abrasivity index for the prediction of ucs and e of misis fault breccia: regression and artificial neural networks analysis. *Expert Systems with Applications*, 37(12):8750–8756. ↑ 32
- Kalender, A., Sonmez, H., Medley, E., Tunusluoglu, C., and Kasapoglu, K. (2014). An approach to predicting the overall strengths of unwelded bimrocks and bimsoils. *Engineering Geology*, 183:65–79. ↑ 31
- Lade, P. V. and Wasif, U. (1988). Effects of height-to-diameter ratio in triaxial specimens on the behavior of cross-anisotropic sand. In *Advanced triaxial testing of soil and rock*. ASTM International. ↑ 36
- Liang, S., Xiao, X., and Feng, D. (2023). Study on large-scale direct shear test on soil–rock mixture in an immersion state under water. *International Journal of Geomechanics*, 23(2):04022294. ↑ 33
- Lindquist, E. and Goodman, R. (1994). Strength and deformation properties of a physical model melange. In *1st North American Rock Mechanics Symposium*. American Rock Mechanics Association. ↑ 31, 32, 33
- Mahdevvari, S. and Moarefvand, P. (2018). Experimental investigation of fractal dimension effect on deformation modulus of an artificial bimrock. *Bull. Eng. Geol. and the Envir.*, 77:1729–1737. ↑ 33
- Medley, E. (1994). Using stereological methods to estimate the volumetric proportions of blocks in melanges and similar block-in-matrix rocks (bimrocks). In *7th International IAEG Congress, Lisboa, Portugal*, pages 1031–1040. ↑ 31
- Medley, E. (2004). Observations on tortuous failure surfaces in bimrocks. *Felsbau, J. of Engineering Geology, Geomechanics and Tunnelling*, 22:35–43. ↑ 31
- Medley, E. and Goodman, R. E. (1994). Estimating the block volumetric proportions of melanges and similar block-in-matrix rocks (bimrocks). In *1st North American Rock Mechanics Symposium*. American Rock Mechanics Association. ↑ 31
- Medley, E. V. and Lindquist, E. S. (1995). The engineering significance of the scale-independence of some franciscan melanges in california, usa. In *The 35th US Symposium on Rock Mechanics (USRMS)*. American Rock Mechanics Association. ↑ 32, 36

- Medley, E. W. (2002a). Estimating block size distributions of melanges and similar block-in-matrix rocks (bimrocks). In *Proc. 5th North American Rock Mechanics Symposium, Toronto, Canada*. ↑ 31
- Medley, E. W. (2002b). Estimating block size distributions of melanges and similar block-in-matrix rocks (bimrocks). In *Proc. 5th North American Rock Mechanics Symposium, Toronto, Canada*. ↑ 32
- Medley, E. W. and Rehermann, P. F. S. (2004). Characterization of bimrocks (rock/soil mixtures) with application to slope stability problems. ↑ 47
- Medley, E. W. and Zekkios, D. (2011). Geopractitioner approaches to working with antisocial mélanges. *Geological Society of America Special Papers*, 480:261–277. ↑ 31, 32
- Miller, E. A. and Sowers, G. F. (1958). The strength characteristics of soil-aggregate mixtures & discussion. *Highway Research Board Bulletin*, 14(183). ↑ 32, 36, 47, 48
- Patwardhan, A., Rao, J., and Gaidhane, R. (1970). Interlocking effects and shearing resistance of boulders and large size particles in a matrix of fines on the basis of large scale direct shear tests. In *Proceedings of the 2nd Southeast Asian Conference on Soil Mechanics, Singapore. Southeast Asian Geotechnical Society, Pathumthani, Thailand*, pages 265–273. ↑ 32
- Ramos-Cañón, A. M., Castro-Malaver, L. C., Padilla-Bello, N. V., and Vega-Posada, C. A. (2020). Incertidumbre en la determinación del porcentaje volumétrico de bloques de bimrocks/bimsoil a partir de información unidimensional. *Boletín de Geología*, 42(1):69–80. ↑ 31
- Rathee, R. (1981). Shear strength of granular soils and its prediction by modeling techniques. *Journal of the Institution of Engineers (India)*, pages 64–70. ↑ 33
- Raymond, L. A. (1984). *Melanges: Their nature, origin, and significance*, volume 198. Geological Society of America. ↑ 31
- Sachan, A. and Penumadu, D. (2007). Effect of microfabric on shear behavior of kaolin clay. *Journal of geotechnical and geoenvironmental engineering*, 133(3):306–318. ↑ 34, 35
- Sharafisafa, M., Aliabadian, Z., Sato, A., and Shen, L. (2024). Effect of strain rate on the failure of bimrocks using the combined finite-discrete element method. *Computers and Geotechnics*, 176:106712. ↑ 33
- Sheikhpourkhani, A., Bahaaddini, M., Oh, J., and Masoumi, H. (2024). Numerical study of the mechanical behaviour of unwelded block in matrix rocks under direct shearing. *Bulletin of Engineering Geology and the Environment*, 83(1):22. ↑ 33

- Sonmez, H., Altinsoy, H., Gokceoglu, C., and Medley, E. (2006). Considerations in developing an empirical strength criterion for bimrocks. In *Proc. 4th Asian Rock Mechanics Symposium, Nov 6-10 2006, Singapore*. ↑ 32, 36
- Wang, S., Zhu, Y., Ma, W., Wang, Z., and Li, G. (2021). Effects of rock block content and confining pressure on dynamic characteristics of soil-rock mixtures. *Eng. Geology*, 280:105963. ↑ 33
- Wang, Y., Que, J., Wang, C., and Li, C. (2018). Three-dimensional observations of meso-structural changes in bimsoil using x-ray computed tomography (ct) under triaxial compression. *Constr Build Mater.*, 190:773–786. ↑ 33
- Wen-Jie, X., Qiang, X., and Rui-Lin, H. (2011). Study on the shear strength of soil–rock mixture by large scale direct shear test. *Int. J. for Rock Mech. and Mining Sciences*, 48(8):1235–1247. ↑ 33
- Zhang, H.-Y., Xu, W.-J., and Yu, Y.-Z. (2016a). Triaxial tests of soil–rock mixtures with different rock block distributions. *Soils Found.*, 56(1):44–56. ↑ 33
- Zhang, L. (2016). *Engineering Properties of Rocks*. Elsevier Science. ↑ 34
- Zhang, Z.-L., Xu, W.-J., Xia, W., and Zhang, H.-Y. (2016b). Large-scale in-situ test for mechanical characterization of soil–rock mixture used in an embankment dam. *Int. J. for Rock Mech. and Mining Sciences*, 86:317–322. ↑ 33

